

## Electron Capture in $\text{He}^{2+}$ Collisions with Aligned $\text{Na}^*(3p)$ Atoms

F. Aumayr, M. Gieler, J. Schweinzer,<sup>(a)</sup> and H. Winter

*Institut für Allgemeine Physik, Technische Universität Wien, Wiedner Hauptstrasse 8-10, A-1040 Wien, Austria*

J. P. Hansen

*Fysisk Institutt, Allegaten 55, N-5000 Bergen, Norway*

(Received 10 January 1992)

State-selective single-electron capture in slow (0.5–3 keV/amu) collisions of  $\text{He}^{2+}$  with laser-excited  $\text{Na}^*(3p)$  atoms has been studied experimentally by means of translational energy spectroscopy, and theoretically by 38-state atomic orbital (AO) close-coupling calculations. The initial orbital alignment of the  $\text{Na}^*(3p)$  state has been controlled via polarization of the exciting laser light. Electron capture into the dominant  $\text{He}^+(n=4)$  state is strongly favored for linear light polarization perpendicular to the  $\text{He}^{2+}$  beam. The impact energy dependence of the observed alignment behavior can be quantitatively explained by the AO calculations.

PACS numbers: 34.70.+e, 34.50.Rk, 82.30.Fi

Optical pumping with linearly polarized laser light permits preparation of excited atoms with well-defined alignment of their magnetic substates (i.e., with an anisotropic charge distribution) as target particles for inelastic collision studies. As compared to spherically symmetric ground-state target atoms, orbital-alignment-dependent collisions can provide additional insight into dynamical processes [1–5].

Recently, Doweck and co-workers have performed collision-spectroscopical studies for aligned as well as oriented  $\text{Na}^*(3p)$  atoms colliding with protons at impact energies between 0.5 and 2 keV [6–10]. Initial-orbital-alignment-dependent effects could be demonstrated [6,8] in agreement with theoretical predictions [11–13].

In this paper we report the first experimental and theoretical studies on the initial-orbital-alignment dependences of doubly charged ions colliding with laser-prepared target atoms. State-selective single-electron capture (SEC) in collisions of  $\text{He}^{2+}$  ions with laser-excited  $\text{Na}^*(3p)$  atoms has been investigated in the impact energy range of 0.5–3 keV/amu, and a pronounced polarization dependence of charge transfer into different final  $\text{He}^+(n)$  states has been found. The measurements have been carried out by means of translational energy spectroscopy, with a setup described in detail in [14,15].  $^4\text{He}^{2+}$  ions produced in a Nier-type ion source were accelerated to 2–12 keV, mass selected by an analyzing magnet, and crossed under  $90^\circ$  with a highly collimated effusive Na beam (for a detailed description see [16]). Charge-exchanged  $\text{He}^+$  ions have been separated from the primary ions by a deceleration lens, and the related translational energy spectra (TES) measured by means of a hemispherical energy analyzer, to determine the involved principal reaction channels.

The TES presented in Figs. 1(a)–1(c) have been measured with an angular acceptance for the  $\text{He}^+$  ions of  $\pm 0.15^\circ$ . Typically 10% of the Na atoms in the target beam could be prepared in the excited  $\text{Na } 3p^2P_{3/2} F=3$  state by pumping with resonant dye laser light ( $\text{NaD}_2$  589 nm) [17]. The chopped laser beam crossed both the

target atom and the ion beam under  $90^\circ$ . Its linear polarization could be rotated within the target-beam-ion-beam plane, permitting spectra to be recorded with laser light polarization directed parallel ( $\parallel$ ) or perpendicular ( $\perp$ ) to the primary ion-beam direction [16]. Using this setup for investigating electron capture in  $\text{He}^{2+}$ - $\text{Na}(3s)/\text{Na}^*(3p)$  collisions, we observed a dramatic difference in  $\text{He}^+$  final-state population due to electron capture from excited  $\text{Na}^*(3p)$  as compared to the  $\text{Na}(3s)$  ground state [17]. With polarization fixed perpendicular to the ion beam, electron capture from  $\text{Na}^*(3p)$  into  $\text{He}^+(n=4)$  and  $\text{He}^+(n=5)$  states was strongly enhanced, whereas capture into  $\text{He}^+(n=3)$ , which is the dominant final state for collisions with  $\text{Na}(3s)$ , decreased significantly. Furthermore, TES for “laser on  $\perp$ ,” “laser on  $\parallel$ ,” and “laser off” have been studied simultaneously by frequently (i.e., in time intervals of 5 s) switching between the three modes, thus averaging over long term ion- and target-beam fluctuations.

Determining the fraction  $f^*$  as described in [17], “pure”  $\text{Na}(3p\perp)$ - and  $\text{Na}(3p\parallel)$ -related TES ( $S^*$ ) could be obtained by appropriate scaling and comparison of the laser on ( $S_{\text{on}}$ ) and laser off ( $S_{\text{off}}$ ) TES signals:

$$S^* = (1/f^*)[S_{\text{on}} - (1 - f^*)S_{\text{off}}].$$

Results for 3 keV/amu impact energy are presented in Figs. 1(a)–1(c).

Figure 1(a) shows TES for collisions with ground-state  $\text{Na}(3s)$  atoms and illustrates the dominance of capture into the  $\text{He}^+(n=3)$  state. Figures 1(b) and 1(c) display TES for capture from excited  $\text{Na}(3p)$  atoms with light polarization parallel (b) and perpendicular (c) to the ion-beam direction, respectively. Although capture into  $\text{He}^+(n=4)$  and  $\text{He}^+(n=5)$  states is also strongly enhanced for  $\text{Na}^*(3p\parallel)$  as compared to  $\text{Na}(3s)$ , a more detailed analysis of the TES in Figs. 1(b) and 1(c) shows that the probability for capture into  $\text{He}^+(n=4)$  decreases if the laser polarization is rotated from perpendicular to parallel to the ion-beam direction, while the oppo-

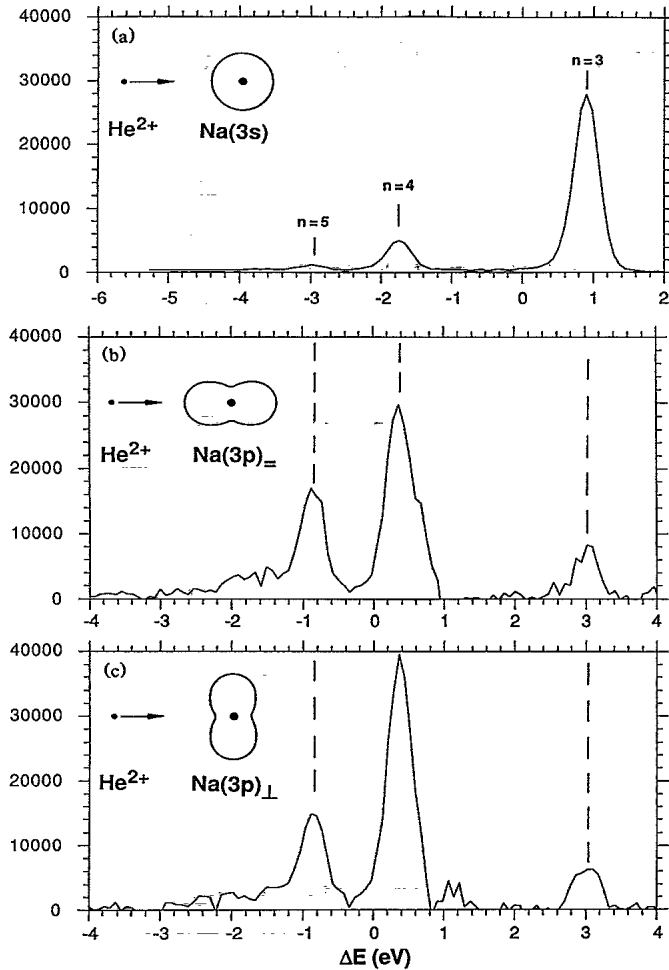


FIG. 1. Translational energy spectra for impact of 3 keV/amu  ${}^4\text{He}^{2+}$  on (a)  $\text{Na}(3s)$ , (b)  $\text{Na}^*(3p)$  with laser light polarization parallel, and (c) perpendicular to the  $\text{He}^{2+}$  beam direction vs the reaction energy defect  $\Delta E$ . The different final  $\text{He}^+(n)$  states for capture from  $\text{Na}(3s)$  and  $\text{Na}^*(3p)$ , respectively, have been indicated by vertical dashed lines.

site was found for capture into both  $\text{He}^+(n=5)$  and  $\text{He}^+(n=3)$  final states. The scattering angle involved in SEC reactions has been estimated by calculations for elastic Coulomb scattering of  $\text{He}^+$  on  $\text{Na}^+$ , at impact parameters leading to the most efficient population of the considered  $\text{He}^+$  final states. Impact parameters related to efficient population of final states were derived from AO (atomic orbital) close-coupling calculations as described below. A comparison of the such derived scattering angles for SEC with the angular acceptance of our TES shows that the latter was sufficiently large to collect all projectiles populating  $\text{He}^+(n=3,4)$  final states. Therefore, the peak areas of TES shown in Figs. 1(a)–1(c) could be evaluated in terms of the (relative) cross sections  $\sigma_{3s}(n=3,4)$ ,  $\sigma_{3p\perp}(n=3,4)$ , and  $\sigma_{3p\parallel}(n=3,4)$ . These relative cross sections have been converted to absolute scale by normalization to cross sections for electron capture into  $\text{He}^+(n=3)$  in  $\text{He}^{2+}$ - $\text{Na}(3s)$  col-

lisions [15,18].

In addition to these experiments we also performed close-coupling calculations with expansion of the time-dependent wave function of the active electron into traveling atomic orbitals [19]. Our basis included  $\text{He}^+(n=2,3,4)$  final projectile states as well as  $\text{Na}(n=3)$  states [an extension of this basis set to include also  $\text{He}^+(n=5)$  states is in progress]. Radial wave functions and the effective potential modeling the interaction of the active electron with the Na core have been taken from [20].

For comparing the experimental and calculated results, suitable relations between measured and calculated quantities have to be established. Linearly polarized laser light, which saturates the  $\text{Na}(3s\ ^2S_{1/2}, F=2 \rightarrow 3p\ ^2P_{3/2}, F=3)$  transition, excites an incoherent mixture of orthogonal  $3p_i$  ( $i=x,y,z$ ) orbitals with relative magnitudes (for ideal pumping) of 2:2:5, the largest component being in the direction of the polarization vector [21]. On the other hand, theoretical results correspond to the preparation of pure  $3p\Sigma$ ,  $3p\Pi^+$ , and  $3p\Pi^-$  atomic orbitals, where  $\Sigma$  and  $\Pi$  label the molecular symmetry of the entrance channel in the  $R \rightarrow \infty$  asymptotic limit. The  $+/-$  signs refer to the symmetry of orbitals with respect to reflection in the collision plane [6]. Since in our measurements the collision plane has not been defined, the cross sections for capture from  $\Pi^+$  and  $\Pi^-$  target states have to be averaged, leading to the cross section  $\sigma_{3p\Pi}$  [7]. The measured and calculated cross sections are thus interrelated by [6]

$$\sigma_{3p\parallel}(n) = \frac{5}{9} \sigma_{3p\Sigma}(n) + \frac{4}{9} \sigma_{3p\Pi}(n),$$

$$\sigma_{3p\perp}(n) = \frac{2}{9} \sigma_{3p\Sigma}(n) + \frac{7}{9} \sigma_{3p\Pi}(n).$$

Experimental results can therefore be unfolded in terms of  $\sigma_{3p\Sigma}(n)$  and  $\sigma_{3p\Pi}(n)$  cross sections. A comparison of experimental and calculated results for  $\sigma_{3p\Sigma}(n=4)$  and  $\sigma_{3p\Pi}(n=4)$  is given in Fig. 2 and shows excellent agreement. The difference in behavior of  $\Sigma$  and  $\Pi$  orbitals is usually described by defining an alignment parameter  $A(n)$  with  $-1 \leq A(n) \leq 1$  [6]:

$$A(n) = \frac{\sigma_{3p\Sigma}(n) - \sigma_{3p\Pi}(n)}{\sigma_{3p\Sigma}(n) + \sigma_{3p\Pi}(n)}.$$

The resulting impact energy dependence of this anisotropy parameter has been compared in Fig. 3 for our experimental and calculated results. Apart from the lowest impact energy, capture into  $\text{He}^+(n=4)$  from  $3p\Pi$  states is almost 3 times more probable than capture from  $3p\Sigma$  states. This situation is different for capture into  $\text{He}^+(n=3)$  and  $\text{He}^+(n=5)$  (the latter has not been shown in Fig. 3, because it has not yet been included in the AO basis). Our theoretical curves agree well with the experimental results. In particular, the energy dependence of  $A(4)$  is fully reproduced. Systematic calculations have been performed with three AO basis sets of different size [AO39:  $\text{Na}(n=3)$ ,  $\text{He}^+(n=1,2,3,4)$ ; AO20:  $\text{Na}(3s,3p)$ ,  $\text{He}^+(n=4)$ ; AO13:  $\text{Na}(3s,3p)$ ,  $\text{He}^+(n=3)$ ]. For capture into  $\text{He}^+(n=4)$  the inclusion of other  $\text{He}^+$  principal

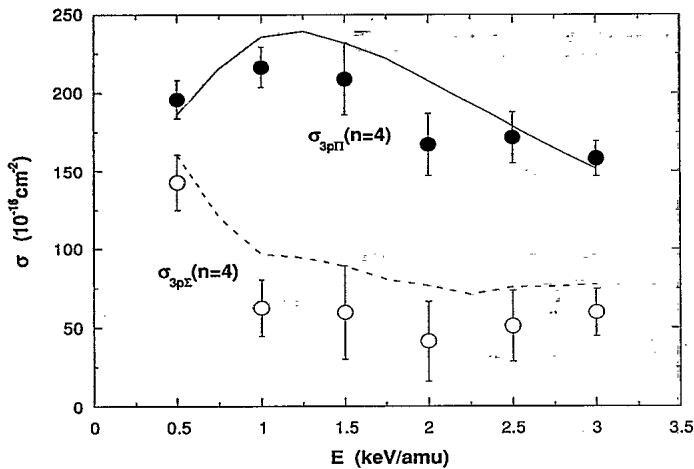


FIG. 2. Absolute experimental and theoretical single-electron capture cross sections in collisions of  ${}^4\text{He}^{2+}$  with  $\text{Na}^*(3p\Sigma)$  and  $\text{Na}^*(3p\Pi)$  into  $\text{He}^+(n=4)$  final states vs ion impact energy. Comparison is made between experimental data (symbols) which have been evaluated from TES with laser light polarized parallel and perpendicular to the ion-beam direction, respectively, and results of the AO calculations (lines).

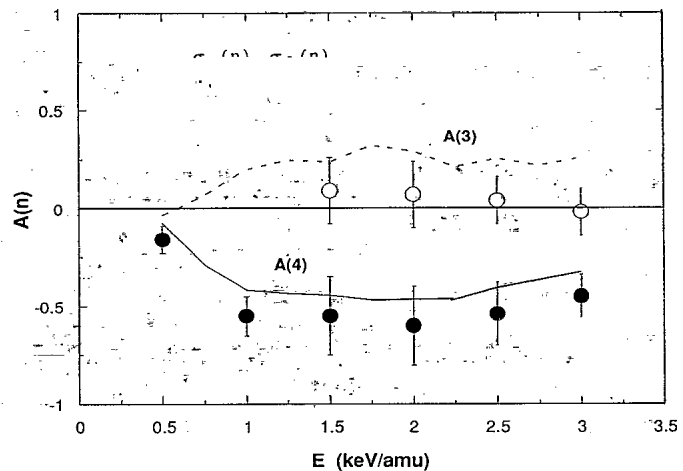


FIG. 3. The  $\Sigma$ - $\Pi$  anisotropy parameter  $A(n)$  for  $\text{He}^+(n=3,4)$  final states plotted vs incident  ${}^4\text{He}^{2+}$  energy. Experimental data (symbols) are compared with the results of our AO calculations (lines).

shells into the basis does not change results for the population of  $\text{He}^+(n=4)$  and especially the  $A(4)$  impact energy dependence, as already seen with the AO20 basis. Therefore, direct electron transfer can be regarded as the predominant mechanism for population of final  $\text{He}^+(n=4)$  states. In Fig. 4 we present impact parameter dependences of the probability  $P(b)$  calculated for capture into all  $\text{He}^+(n=4)$  final states from  $\text{Na}^*(3p\Sigma)$ ,  $\text{Na}^*(3p\Pi^+)$ , and  $\text{Na}^*(3p\Pi^-)$ , respectively (AO39 basis; 1 keV/amu impact energy). Electron transfer from  $\text{Na}^*(3p)$  to  $\text{He}^+(n=4)$  final states becomes more and more likely with increasing internuclear distance because of the decreasing energy splitting between corresponding diabatic potential-energy curves, as long as the coupling remains sufficiently strong. Therefore, the different geometrical shapes of the  $3p\Sigma$  and  $3p\Pi^+$  charge clouds with respect to the projectile trajectory determine in a simple manner the capture probability in collisions involving  $b \geq 15a_0$ . In other words, at larger impact parameters  $b$  (cf. Fig. 4) capture from  $3p\Pi^+$  can proceed more efficiently than capture from  $3p\Sigma$ , because of the enhanced coupling strength resulting from an increased overlap between the initial target and final projectile states for  $3p\Pi^+$ . This dramatic effect is partially reduced, however, by a comparably low capture probability from  $3p\Pi^-$  (i.e., a  $p$  orbital extending out of the collision plane), which has to be averaged with the  $3p\Pi^+$  related data to correspond to the experimentally prepared  $3p\Pi$  state (see above). For capture into  $\text{He}^+(n=3)$ , our simple picture does not hold, since our calculations show that electron transfer takes place at considerably smaller internuclear distances than  $15a_0$ . There, initially differently aligned charge clouds lead to different overlap

and potential coupling elements which have a complex effect on the resulting capture probability in our AO calculations. Moreover, interaction with other final  $\text{He}^+(n)$  states is more pronounced for this weak capture channel (AO13 compared with AO39 basis).

In conclusion, a strong effect of the initial target atom alignment for electron capture in collisions of 0.5–3-keV/amu  $\text{He}^{2+}$  ions with laser-excited  $\text{Na}^*(3p)$  atoms has been found. The experimental results can be satisfactorily reproduced in the framework of atomic orbital expansion close-coupling calculations. A simple interpretation in terms of capture probability in direct relation to

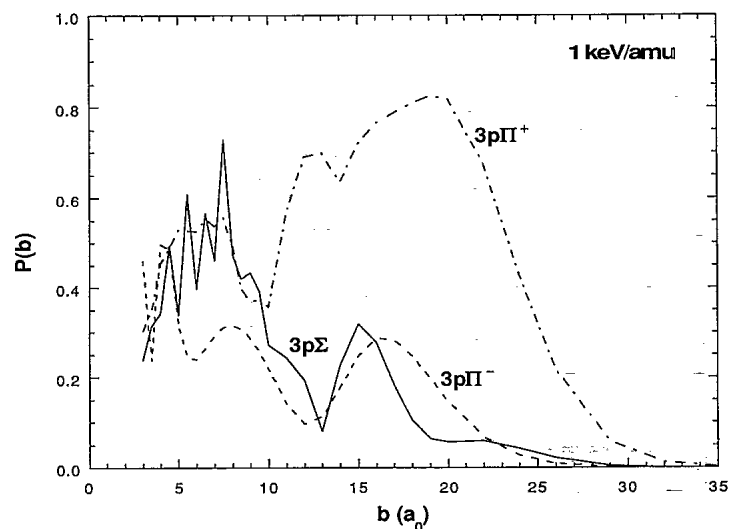


FIG. 4. Calculated impact parameter dependence of the probabilities  $P(b)$  for capture into all  $\text{He}^+(n=4)$  final states from  $\text{Na}(3p\Sigma)$ ,  $\text{Na}(3p\Pi^+)$ , and  $\text{Na}(3p\Pi^-)$ , respectively ( ${}^4\text{He}^{2+}$  impact energy 1 keV/amu).

the charge cloud density of the initial state along the trajectory explains the alignment parameter  $A(4)$  very well. However, this geometrical picture cannot be generally applied to other collision systems; cf. the results of Doweck *et al.* [6] for the dominant  $H(n=2)$  capture channel in  $H^+ - Na^*(3p\Sigma, 3p\Pi)$  collisions. The complex influence of the shape of the charge cloud on electron capture might be understood in more detail, when following the electron charge cloud development along the collisional trajectory [8]. Corresponding studies are in progress.

This work has been supported by Fonds zur Förderung der wissenschaftlichen Forschung (Projekt No. 7006) and by Kommission zur Koordination der Kernfusionsforschung at the Austrian Academy of Sciences. The authors also thank Mr. W. Koppensteiner (IAP) and Dr. K. Lozhkin (A. F. Ioffe Institute, St. Petersburg) for participation in the measurements.

<sup>(a)</sup>Present address: Max Planck Institut für Plasmaphysik, D-8046 Garching, Germany.

- [1] I. V. Hertel and W. Stoll, *Adv. At. Mol. Phys.* **13**, 113 (1978).
- [2] A. Bähring, I. V. Hertel, E. Meyer, and H. Schmidt, *Z. Phys. A* **312**, 293 (1983).
- [3] I. V. Hertel, H. Schmidt, H. Bähring, and E. Meyer, *Rep. Prog. Phys.* **48**, 375 (1985).
- [4] E. E. B. Campbell and I. V. Hertel, *Adv. Chem. Phys.* **72**, 37 (1988).
- [5] R. Witte, E. E. B. Campbell, C. Richter, H. Schmidt, and I. V. Hertel, *Z. Phys. D* **5**, 101 (1987).
- [6] D. Doweck, J. C. Houver, J. Pommier, C. Richter, and T. Royer, *Phys. Rev. Lett.* **64**, 1713 (1990).
- [7] T. Royer, D. Doweck, J. C. Houver, J. Pommier, and N. Andersen, *Z. Phys. D* **10**, 45 (1988).
- [8] C. Richter, D. Doweck, J. C. Houver, and N. Andersen, *J. Phys. B* **23**, 3925 (1990).
- [9] K. Finck, Y. Wang, Z. Roller-Lutz, and H. O. Lutz, *Phys. Rev. A* **38**, 6115 (1988).
- [10] D. Doweck, J. C. Houver, and C. Richter, in *Proceedings of the Seventeenth International Conference on the Physics of Electronic and Atomic Collisions, Brisbane, Australia, 1991* (to be published).
- [11] R. J. Allan, R. Shingal, and D. R. Flower, *J. Phys. B* **19**, L251 (1986).
- [12] W. Fritsch (private communication); data cited in Courbin *et al.* (Ref. [13]).
- [13] C. Courbin, R. J. Allan, P. Salas, and P. Wahnon, *J. Phys. B* **23**, 3909 (1990).
- [14] F. Aumayr, J. Schweinzer, and H. Winter, *J. Phys. B* **22**, 1027 (1989).
- [15] J. Schweinzer and H. Winter, *J. Phys. B* **23**, 3881 (1990).
- [16] M. Gieler, F. Aumayr, M. Hütteneder, and H. Winter, *J. Phys. B* **24**, 4419 (1991).
- [17] F. Aumayr, M. Gieler, E. Unterreiter, and H. Winter, *Europhys. Lett.* **16**, 557 (1991).
- [18] For impact energies  $> 6$  keV no experimental data were available for normalization. Therefore, results of our AO calculations, which are in excellent agreement with experimental results of [15] for impact energies  $\leq 6$  keV, have been used for normalization in the impact energy range 6–12 keV.
- [19] S. E. Nielsen, J. P. Hansen, and A. DuBois, *J. Phys. B* **23**, 2595 (1990).
- [20] D. Rapp and C. Chang, *J. Chem. Phys.* **58**, 2657 (1973).
- [21] A. Fischer and I. V. Hertel, *Z. Phys. A* **304**, 103 (1982).